Nuclear Science and Techniques (2025) 36:8
https://doi.org/10.1007/s41365-024-01570-7

A novel method for simultaneous measurement of ^{222}Rn and ^{220}Rn progeny concentrations measured by an alpha spectrometer

Zhong-Kai Fan[1,2] · Jia-Le Sun[2] · Hao-Xuan Li[1] · Xiang-Ming Cai[1] · Hui Yang[1] · Shou-Kang Qiu[1] · Yan-Liang Tan[2] · Jian Shan[1]

Received: 25 March 2024 / Revised: 21 April 2024 / Accepted: 23 April 2024 / Published online: 18 December 2024

Abstract

The accumulation of ^{222}Rn and ^{220}Rn progeny in poorly ventilated environments poses the risk of natural radiation exposure to the public. A previous study indicated that satisfactory results in determining the ^{222}Rn and ^{220}Rn progeny concentrations by measuring the total alpha counts at five time intervals within 560 min should be expected only in the case of high progeny concentrations in air. To complete the measurement within a relatively short period and adapt it for simultaneous measurements at comparatively lower ^{222}Rn and ^{220}Rn progeny concentrations, a novel mathematical model was proposed based on the radioactive decay law. This model employs a nonlinear fitting method to distinguish nuclides with overlapping spectra by utilizing the alpha particle counts of non-overlapping spectra within consecutive measurement cycles to obtain the concentrations of ^{222}Rn and ^{220}Rn progeny in air. Several verification experiments were conducted using an alpha spectrometer. The experimental results demonstrate that the concentrations of ^{222}Rn and ^{220}Rn progeny calculated by the new method align more closely with the actual circumstances than those calculated by the total count method, and their relative uncertainties are all within ± 16%. Furthermore, the measurement time was reduced to 90 min, representing an acceleration of 84%. The improved capability of the new method in distinguishing alpha particles with similar energies emitted from ^{218}Po and ^{212}Bi, both approximately 6 MeV, contributed to realizing more accurate results. The proposed method has the potential advantage of measuring relatively low concentrations of ^{222}Rn and ^{220}Rn progeny in air more quickly via air filtration.

Keywords ^{222}Rn · ^{220}Rn · Progeny concentration · Nonlinear fitting method · Alpha spectrometer

1 Introduction

Radioactive gases ^{222}Rn and ^{220}Rn are colorless, tasteless, and odorless. They are universally present in the walls, floors, and ceilings of buildings, as well as in the surrounding soil, before permeating into the cracks of a building and entering indoor spaces [1, 2]. Their decay products typically accumulate in closed spaces or poorly ventilated areas such as basements, mines, and warehouses [3, 4]. The generated progeny atoms recombine with air ions and other air impurity clusters to form clusters of size 0.5 nm − 5 nm, which are referred to as radioactive unattached particles [5–7]. After this process, the clusters attach to submicron-sized aerosol particles in the air within 1–100 s, forming radioactive aerosols or attached particles with sizes ranging from 100 nm to 500 nm [8, 9]. During breathing, radioactive progeny aerosols are inhaled into the respiratory organs. Some aerosols remain adsorbed in the respiratory system, where they continue to undergo radioactive decay [10]. During this process, the progeny of ^{222}Rn and ^{220}Rn can cause continuous tissue damage, leading to lung cancer. The inhalation doses are contributed by their progeny, but not by the gas itself [11]. Therefore, numerous researchers conducted

This work was supported by the National Natural Science Foundation of China (No. 12075112), Natural Science Foundation of Hunan (No. 2023JJ50121), Natural Science Foundation of Hunan Province (No. 2023JJ50091), and Key Projects of Hunan Provincial Department of Education (No. 23A0516).

✉ Jian Shan
shanjian0666@163.com

[1] School of Nuclear Science and Technology, University of South China, Hengyang 421001, China

[2] College of Physics and Electronic Engineering, Hengyang Normal University, Hengyang 421008, China

studies on detectors for measuring ^{222}Rn and ^{220}Rn progeny concentrations.

Various detectors have been developed for measuring alpha particles emitted from ^{222}Rn and ^{220}Rn progeny in air, including ZnS(Ag)-coated scintillation cells [12, 13], the imaging plate (IP) [14], solid-state nuclear track detectors (SSNTD) [15, 16], silicon semiconductor detectors [17, 18], and others. An alpha spectrometer, equipped with ULTRA ion-implanted silicon semiconductor detectors, features a high-energy resolution, low background, and appropriate detection efficiency. Therefore, it is frequently employed for the identification and quantitative analysis of mixtures of radionuclides based on the alpha particles emitted during decay [19, 20].

Previously, methods based on air filtration followed by measurements using an alpha spectrometer have been widely explored for the determination of mixed ^{222}Rn and ^{220}Rn progenies in environmental air [21–25]. Harley et al. proposed a method that includes a 60-min sampling period, with counts considered at five intervals within 2440 min, to estimate the individual concentrations of ^{222}Rn and ^{220}Rn progeny. Hence, the lung dose due to ^{220}Rn progeny [21] is assessed. A comparable method employed in high-background areas in Yangjiang County, China, involved 30-min sampling, followed by five measurement intervals within 560 min, and ensuring on-site measurement work completion within ten hours [22]. For more accurate measurement of the concentrations of mixed ^{222}Rn and ^{220}Rn progeny, a set of optimum time intervals was obtained by comparing the uncertainties in the total alpha spectroscopy data across the three sets of measurement intervals. Each set of time intervals lasted 560 min and was calculated using the weighted least-squares method [23]. To assess the reliability of this air filtration method, the sensitivity of the measurements of ^{222}Rn and ^{220}Rn concentrations in air to variations in alpha counting at three and five intervals (560 min) was examined [24]. They indicated that the ^{222}Rn progeny reached saturation activities on the filter after 3 h of filtering, whereas the saturation activities of ^{220}Rn were achieved after three days owing to the different half-lives in the ^{220}Rn chain. The influences of ^{222}Rn and ^{220}Rn concentrations, filtering duration, and choice of measuring interval (560 min) on the relative standard deviations were further analyzed [25]. Their study indicated that satisfactory results using the total count method should be expected only in the case of high radon and thoron progeny concentrations in air.

In contrast to the total alpha-counting method, which requires five counting intervals, the alpha spectroscopy method enables the direct differentiation of alpha particles with varying energies emitted by ^{218}Po, ^{214}Po, ^{212}Bi, and ^{212}Po. This is widely preferred, particularly in the context of modern requirements for high measurement accuracy [26–29]. In 1978, Kerr introduced an α spectrometry technique to measure the activity concentration of short-lived radon and thoron progenies. This method, termed as Kerr-Tn, utilizes an inverse matrix and obtains five alpha counts within the region of interest (ROI). Three counting intervals were established, each with a sampling time of 10 min: 2–12 min, 15–30 min, and 200–220 min. The intervals were initiated after the completion of sample collection [30]. Compared to the Kerr-Tn method, both the PKU-Tn and Wicke-Tn methods exhibit the advantage of synchronizing the first counting interval with the sampling time. With an extended 30-min sampling time and a total measurement duration of 180 min, this results in an increase in methodological sensitivity by nearly 8.97 times and 3.56 times, respectively [31]. However, adopting a method of simultaneous sampling and measurement may lead to broadening of the measured alpha energy spectrum because there is a need for a distance between the detector and filter membrane to allow for gas circulation. This in turn affects the accuracy of the measurements [32]. Furthermore, previous fitting methods demonstrated significant advantages in alpha energy spectrum measurements. For the deconvolution of the alpha particle spectra, improved peak shape formulae were implemented as fit functions in a spreadsheet application, and the optimum fit parameters were searched using built-in optimization routines [33]. Considering the entire spectrum background, background noise, and peaks with low statistical counts, a model was developed by fitting the typical shape of the alpha peak [34].

To complete the measurement within a relatively short period of time and adapt to simultaneous measurements at comparatively lower ^{222}Rn and ^{220}Rn progeny concentrations, a new mathematical model based on the radioactive decay law was proposed by performing a nonlinear fitting on the counts of alpha particles with different energies over continuous measurement periods to deduce the concentrations of ^{222}Rn and ^{220}Rn progeny in air. Several measurements were taken using the alpha spectrometer. The results of the proposed method are then compared with those of the total count method [25]. This indicates that the newly proposed method shows more potential advantages in the fast simultaneous measurement of relatively low concentrations of ^{222}Rn and ^{220}Rn progeny in air.

2 Materials and methods

2.1 Alpha emitter from ^{222}Rn and ^{220}Rn progeny

The decay chains of ^{222}Rn and ^{220}Rn are shown in Fig. 1 [35, 36], excluding branches with a low probability. There are some short-lived alpha emitters of radon and thoron progeny

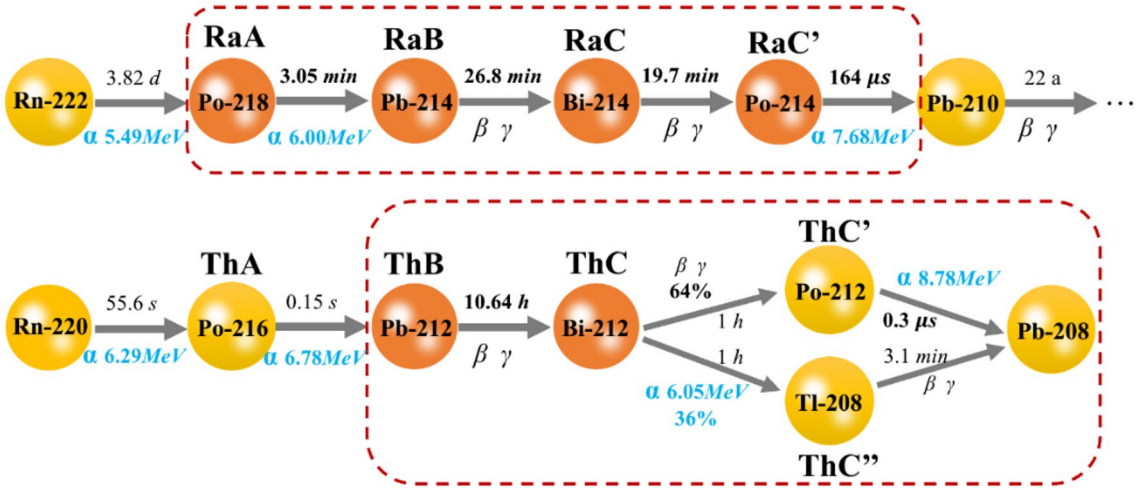

Fig. 1 (Color online) Decay chains of ^{222}Rn and ^{220}Rn

in the air, including RaA (^{218}Po, 6.0 MeV), RaC' (^{214}Po, 7.69 MeV), ThA (^{216}Po, 6.78 MeV), ThC (^{212}Bi, 6.05 MeV), and ThC' (^{212}Po, 8.78 MeV). Given the air filtration method employed in this study, progeny with extremely short half-lives, such as ^{214}Po and ^{212}Po, quickly reaches equilibrium with their parents during the sampling process. Additionally, it is assumed that ^{212}Pb originates directly from ^{220}Rn due to the short half-life of ^{216}Po. In reality, ^{212}Bi emits an alpha only 36% of the time, whereas the remaining 64% of the time it emits a beta. This is followed almost immediately by an alpha through the decay of ^{212}Po (with a half-life of 0.3 s). Furthermore, ^{212}Po decays with an alpha energy of 8.78 MeV and ^{208}Tl decays via beta decay only. It is impossible to distinguish the activity on the filter because of 6.05 MeV alpha particles from ThC and 6.0 MeV alpha particles from RaA. However, the activity can be partitioned between RaA and ThC using the 8.78 MeV alpha particle activity from ThC' [30].

2.2 Measurement method of the progeny of ^{222}Rn and ^{220}Rn via alpha spectroscopy

The new method of simultaneously measuring the progeny concentrations of ^{222}Rn and ^{220}Rn by using an alpha spectrometer includes three time intervals: sampling duration (T_1), time interval (T_2) between the end of sampling and beginning of the measuring the progeny of ^{222}Rn and ^{220}Rn on the filter membrane, and time duration (T_3) for alpha spectrometer measurements from the beginning to the end. Three assumptions are made: (1) the flow rate remains steady during the sampling process; (2) the concentrations of RaA, RaB, RaC, ThB, and ThC in the environment remain constant throughout the sampling process; and (3) the filter exhibits the same collection efficiency for different ^{222}Rn/^{220}Rn progenies, and its self-absorption can be considered negligible. This procedure is illustrated in Fig. 2 and can be described as follows:

2.2.1 Sampling

Before the sampling begins, the number of atoms in ^{222}Rn and ^{220}Rn progenies on the filter membrane is zero. The switch of the vacuum pump is turned on to draw air containing the progeny of ^{222}Rn and ^{220}Rn into the sampler through a flow meter, where ^{222}Rn and ^{220}Rn are collected on the filter. Subsequently, air is returned to the chamber with mixed concentrations of ^{222}Rn and ^{220}Rn. The sampling duration lasts for fifteen minutes. During the sampling process, the quantity of ^{222}Rn and ^{220}Rn progeny on the filter membrane continuously increases. However, this quantity also decreases owing to the decay of parent nuclides and their decay. This can be expressed using the following system of differential equations.

$$\begin{cases} \mathrm{d}N_{\mathrm{RaA}}/\mathrm{d}t = QGC_{\mathrm{RaA}}/\lambda_{\mathrm{RaA}} - N_{\mathrm{RaA}}\lambda_{\mathrm{RaA}} \\ \mathrm{d}N_{\mathrm{RaB}}/\mathrm{d}t = QGC_{\mathrm{RaB}}/\lambda_{\mathrm{RaB}} + N_{\mathrm{RaA}}\lambda_{\mathrm{RaA}} - N_{\mathrm{RaB}}\lambda_{\mathrm{RaB}} \\ \mathrm{d}N_{\mathrm{RaC}}/\mathrm{d}t = QGC_{\mathrm{RaC}}/\lambda_{\mathrm{RaC}} + N_{\mathrm{RaB}}\lambda_{\mathrm{RaB}} - N_{\mathrm{RaC}}\lambda_{\mathrm{RaC}} \\ \mathrm{d}N_{\mathrm{ThB}}/\mathrm{d}t = QGC_{\mathrm{ThB}}/\lambda_{\mathrm{ThB}} - N_{\mathrm{ThB}}\lambda_{\mathrm{ThB}} \\ \mathrm{d}N_{\mathrm{ThC}}/\mathrm{d}t = QGC_{\mathrm{ThC}}/\lambda_{\mathrm{ThC}} + N_{\mathrm{ThB}}\lambda_{\mathrm{ThB}} - N_{\mathrm{ThC}}\lambda_{\mathrm{ThC}} \end{cases} \quad (1)$$

where G is the filtration efficiency, Q is the flow rate, C_{RaA}, C_{RaB}, C_{RaC}, C_{ThB}, and C_{ThC} are the activity concentrations of RaA, RaB, RaC, ThB, and ThC, respectively. λ_{RaA}, λ_{RaB}, λ_{RaC}, λ_{ThB}, and λ_{ThC} are decay constants. N_{RaA}, N_{RaB}, N_{RaC}, N_{ThB}, and N_{ThC} are the number of atoms of RaA, RaB, RaC, ThB, and ThC on the filter membrane during the sampling process.

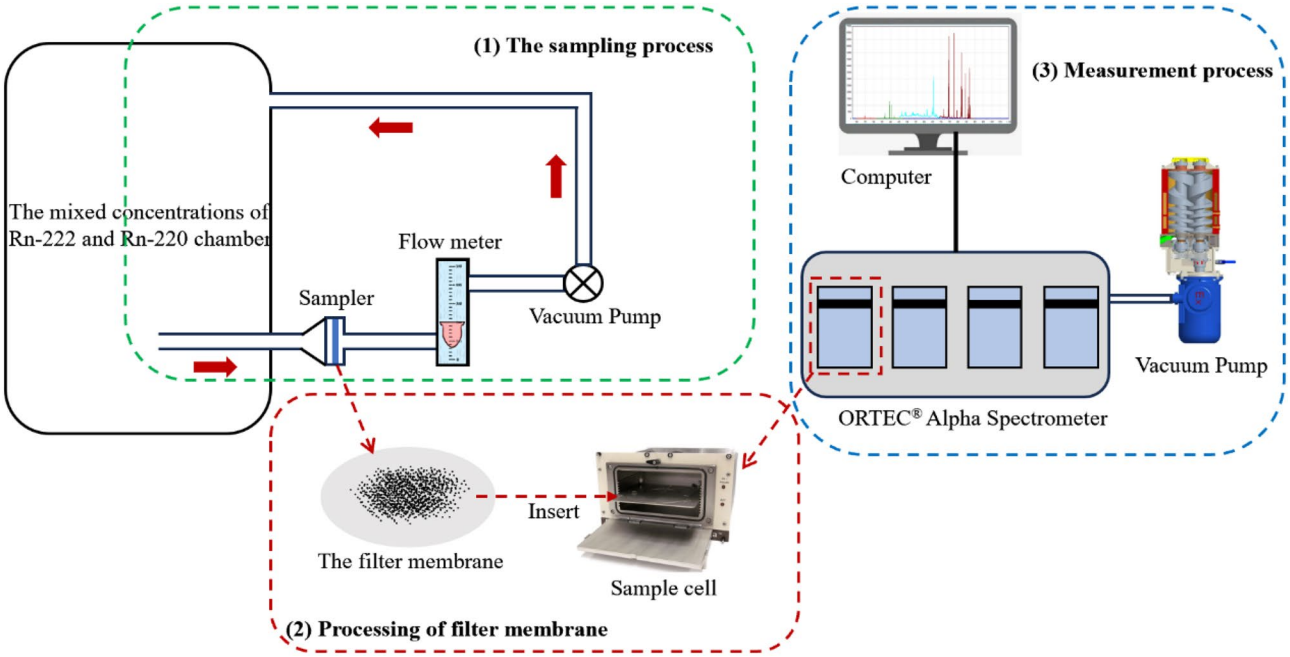

Fig. 2 (Color online) Process of simultaneously measuring the progeny concentrations of ^{222}Rn and ^{220}Rn using the alpha spectrometer

The solution to Eq. (1) shows the relationship between the accumulated number of atoms of RaA, RaB, RaC, ThB, and ThC on the filter membrane at the end of the sampling time T_1 and the activity concentrations of RaA, RaB, RaC, ThB, and ThC in air.

2.2.2 Filter membrane processing

After completing the sampling, the filter membrane was removed and placed in the sample cell of the alpha spectrometer for measurement with a one-minute time interval. In this process, the ^{220}Rn gas did not remain on the filter membrane, and its progeny ^{216}Po on the filter membrane completely decayed. Therefore, there was no spectral interference from the alpha particles emitted by the decay of ^{222}Rn and ^{216}Po during the measurement. At the end of sampling, the quantity of progeny of ^{222}Rn and ^{220}Rn on the filter membrane began to decrease because of decay. Meanwhile, the quantity of progeny nuclides also increases owing to the decay of the parent nuclides. This can be expressed by the following differential equation:

$$\begin{cases} \mathrm{d}N_{\mathrm{RaA1}}/\mathrm{d}t = -N_{\mathrm{RaA1}}\lambda_{\mathrm{RaA}} \\ \mathrm{d}N_{\mathrm{RaB1}}/\mathrm{d}t = N_{\mathrm{RaA1}}\lambda_{\mathrm{RaA}} - N_{\mathrm{RaB1}}\lambda_{\mathrm{RaB}} \\ \mathrm{d}N_{\mathrm{RaC1}}/\mathrm{d}t = N_{\mathrm{RaB1}}\lambda_{\mathrm{RaB}} - N_{\mathrm{RaC1}}\lambda_{\mathrm{RaC}} \\ \mathrm{d}N_{\mathrm{ThB1}}/\mathrm{d}t = -N_{\mathrm{ThB1}}\lambda_{\mathrm{ThB}} \\ \mathrm{d}N_{\mathrm{ThC1}}/\mathrm{d}t = N_{\mathrm{ThB1}}\lambda_{\mathrm{ThB}} - N_{\mathrm{ThC1}}\lambda_{\mathrm{ThC}} \end{cases} \quad (2)$$

where N_{RaA1}, N_{RaB1}, N_{RaC1}, N_{ThB1}, and N_{ThC1} denote the number of atoms of RaA, RaB, RaC, ThB, and ThC, respectively, on the filter membrane during time interval T_2.

The solution to Eq. (2) establishes a relationship between the number of atoms of RaA, RaB, RaC, ThB, and ThC on the filter membrane at time T_2 and the number of atoms of RaA, RaB, RaC, ThB, and ThC at the end of the sampling period.

2.2.3 Measurement process

After processing, the filter membrane was sent to the internal cell of an alpha spectrometer. The alpha spectrometer was connected to a computer via a data cable, and the measured counts of different alpha particles under a vacuum pressure below 1000 mTorr were displayed in real time using MAESTRO software on the computer. At the beginning of alpha spectrometer measurement on the filter membrane, the number of atoms of RaA, RaB, RaC, ThB, and ThC on the filter membrane are represented as N_{RaA2}, N_{RaB2}, N_{RaC2}, N_{ThB2}, and N_{ThC2}, respectively. According to Eqs. (1 and 2), the activity concentrations of RaA, RaB, RaC, ThB, and ThC in air can be deduced. After the alpha spectrometer measurement was initiated, the progeny of ^{222}Rn and ^{220}Rn on the filter membrane continues to decay according to Eq. 2. During the measurement process, the number of RaA, RaB, RaC, ThB, and ThC atoms on the filter membrane at any given time t

are represented as N_{RaA3}, N_{RaB3}, N_{RaC3}, N_{ThB3}, and N_{ThC3}, respectively, and they can be determined as follows:

$$N_{\mathrm{RaA3}}(t) = N_{\mathrm{RaA2}} e^{-\lambda_{\mathrm{RaA}} t} \tag{3}$$

$$N_{\mathrm{RaB3}}(t) = \frac{\lambda_{\mathrm{RaA}} N_{\mathrm{RaA2}} e^{-\lambda_{\mathrm{RaA}} t}}{\lambda_{\mathrm{RaB}} - \lambda_{\mathrm{RaA}}} - \left(\frac{\lambda_{\mathrm{RaA}} N_{\mathrm{RaA2}}}{\lambda_{\mathrm{RaB}} - \lambda_{\mathrm{RaA}}} - N_{\mathrm{RaB2}} \right) e^{-\lambda_{\mathrm{RaB}} t} \tag{4}$$

$$\begin{aligned} N_{\mathrm{RaC3}}(t) = & \frac{-\left(\frac{\lambda_{\mathrm{RaA}} N_{\mathrm{RaA2}}}{\lambda_{\mathrm{RaB}} - \lambda_{\mathrm{RaA}}} - N_{\mathrm{RaB2}} \right) \lambda_{\mathrm{RaB}} e^{-\lambda_{\mathrm{RaB}} t}}{\lambda_{\mathrm{RaC}} - \lambda_{\mathrm{RaB}}} \\ & + \frac{\frac{N_{\mathrm{RaA2}}}{\lambda_{\mathrm{RaB}} - \lambda_{\mathrm{RaA}}} \lambda_{\mathrm{RaA}} \lambda_{\mathrm{RaB}} e^{-\lambda_{\mathrm{RaA}} t}}{\lambda_{\mathrm{RaC}} - \lambda_{\mathrm{RaA}}} \\ & + \left[N_{\mathrm{RaC2}} + \frac{\left(\frac{\lambda_{\mathrm{RaA}} N_{\mathrm{RaA2}}}{\lambda_{\mathrm{RaB}} - \lambda_{\mathrm{RaA}}} - N_{\mathrm{RaB2}} \right) \lambda_{\mathrm{RaB}}}{\lambda_{\mathrm{RaC}} - \lambda_{\mathrm{RaB}}} - \frac{\frac{\lambda_{\mathrm{RaA}} N_{\mathrm{RaA2}}}{\lambda_{\mathrm{RaB}} - \lambda_{\mathrm{RaA}}} \lambda_{\mathrm{RaB}}}{\lambda_{\mathrm{RaC}} - \lambda_{\mathrm{RaA}}} \right] e^{-\lambda_{\mathrm{RaC}} t} \end{aligned} \tag{5}$$

$$N_{\mathrm{ThB3}}(t) = N_{\mathrm{ThB2}} e^{-\lambda_{\mathrm{ThB}} t} \tag{6}$$

$$N_{\mathrm{ThC3}}(t) = \frac{\lambda_{\mathrm{ThB}} N_{\mathrm{ThB2}} e^{-\lambda_{\mathrm{ThB}} t}}{\lambda_{\mathrm{ThC}} - \lambda_{\mathrm{ThB}}} - \left(\frac{N_{\mathrm{ThB2}} \lambda_{\mathrm{ThB}}}{\lambda_{\mathrm{ThC}} - \lambda_{\mathrm{ThB}}} - N_{\mathrm{ThC2}} \right) e^{-\lambda_{\mathrm{ThC}} t} \tag{7}$$

The number of atoms of RaA, RaB, RaC, ThB, and ThC on the filter membrane in Eqs. (8, 9, 10, 11, 12) into their respective activity forms:

$$A_{\mathrm{RaA}}(t) = \lambda_{\mathrm{RaA}} N_{\mathrm{RaA2}} e^{-\lambda_{\mathrm{RaA}} t} \tag{8}$$

$$A_{\mathrm{RaB}}(t) = \lambda_{\mathrm{RaB}} \left[\frac{\lambda_{\mathrm{RaA}} N_{\mathrm{RaA2}} e^{-\lambda_{\mathrm{RaA}} t}}{\lambda_{\mathrm{RaB}} - \lambda_{\mathrm{RaA}}} - \left(\frac{\lambda_{\mathrm{RaA}} N_{\mathrm{RaA2}}}{\lambda_{\mathrm{RaB}} - \lambda_{\mathrm{RaA}}} - N_{\mathrm{RaB2}} \right) e^{-\lambda_{\mathrm{RaB}} t} \right] \tag{9}$$

$$\begin{aligned} A_{\mathrm{RaC}}(t) = \lambda_{\mathrm{RaC}} \Bigg\{ & \frac{-\left(\frac{\lambda_{\mathrm{RaA}} N_{\mathrm{RaA2}}}{\lambda_{\mathrm{RaB}} - \lambda_{\mathrm{RaA}}} - N_{\mathrm{RaB2}} \right) \lambda_{\mathrm{RaB}} e^{-\lambda_{\mathrm{RaB}} t}}{\lambda_{\mathrm{RaC}} - \lambda_{\mathrm{RaB}}} \\ & + \frac{\frac{N_{\mathrm{RaA2}}}{\lambda_{\mathrm{RaB}} - \lambda_{\mathrm{RaA}}} \lambda_{\mathrm{RaA}} \lambda_{\mathrm{RaB}} e^{-\lambda_{\mathrm{RaA}} t}}{\lambda_{\mathrm{RaC}} - \lambda_{\mathrm{RaA}}} \\ & + \left[N_{\mathrm{RaC2}} + \frac{\left(\frac{\lambda_{\mathrm{RaA}} N_{\mathrm{RaA2}}}{\lambda_{\mathrm{RaB}} - \lambda_{\mathrm{RaA}}} - N_{\mathrm{RaB2}} \right) \lambda_{\mathrm{RaB}}}{\lambda_{\mathrm{RaC}} - \lambda_{\mathrm{RaB}}} - \frac{\frac{\lambda_{\mathrm{RaA}} N_{\mathrm{RaA2}}}{\lambda_{\mathrm{RaB}} - \lambda_{\mathrm{RaA}}} \lambda_{\mathrm{RaB}}}{\lambda_{\mathrm{RaC}} - \lambda_{\mathrm{RaA}}} \right] e^{-\lambda_{\mathrm{RaC}} t} \Bigg\} \end{aligned} \tag{10}$$

$$A_{\mathrm{ThB}}(t) = \lambda_{\mathrm{ThB}} N_{\mathrm{ThB2}} e^{-\lambda_{\mathrm{ThB}} t} \tag{11}$$

$$A_{\mathrm{ThC}}(t) = \lambda_{\mathrm{ThC}} \left[\frac{\lambda_{\mathrm{ThB}} N_{\mathrm{ThB2}} e^{-\lambda_{\mathrm{ThB}} t}}{\lambda_{\mathrm{ThC}} - \lambda_{\mathrm{ThB}}} - \left(\frac{N_{\mathrm{ThB2}} \lambda_{\mathrm{ThB}}}{\lambda_{\mathrm{ThC}} - \lambda_{\mathrm{ThB}}} - N_{\mathrm{ThC2}} \right) e^{-\lambda_{\mathrm{ThC}} t} \right] \tag{12}$$

During the alpha spectrometer measurements, the activities of RaA, RaB, RaC, ThB, and ThC on the filter membrane are denoted as A_{RaA}, A_{RaB}, A_{RaC}, A_{ThB}, and A_{ThC}, respectively. Distinguishing between the activity on the filter attributed to 6.05 MeV alpha particles from ThC and 6.0 MeV alpha particles from RaA is unfeasible. However, the activity can be apportioned between RaA and ThC by utilizing 8.78 MeV alpha particle emissions originating from ThC'. According to the radioactive decay characteristics of ^{222}Rn and ^{220}Rn, the alpha particle counts of 8.78 MeV characteristic peak originate from $0.64 \times A_{\mathrm{ThC}}$; the alpha particle counts of the 7.69 MeV characteristic peak originate from A_{RaC}; and the alpha particle counts of the 6.0 MeV characteristic peak originate from $A_{\mathrm{RaA}} + 0.36 \times A_{\mathrm{ThC}}$.

Short measurement cycles were implemented with a measurement period T, and there are i measurement cycles. The total measurement time is T_3. In the ith measurement cycle, the net alpha counts are obtained in their respective alpha spectrum of regions of interest, denoted by ROI-1 (8.78 MeV), ROI-2 (7.69 MeV), and ROI-3 (6.0 MeV), and they can be represented by $n_{\mathrm{ThC}}(i)$, $n_{\mathrm{RaC}}(i)$, and $n_{\mathrm{RaA+ThC}}(i)$. Owing to the short duration of each measurement cycle, the average counts for the ith measurement cycle are approximately equal to the values of A_{ThC}, A_{RaC}, and A_{RaA} at the midpoint of the measurement cycle, and they can be expressed as:

$$\begin{aligned} \frac{n_{\mathrm{ThC}}(i)}{T} &= 0.64 E A_{\mathrm{ThC}} \left(iT - \frac{1}{2} T \right) \\ &= 0.64 E \lambda_{\mathrm{ThC}} \left[\frac{\lambda_{\mathrm{ThB}} N_{\mathrm{ThB2}} e^{-\lambda_{\mathrm{ThB}} \left(iT - \frac{1}{2} T \right)}}{\lambda_{\mathrm{ThC}} - \lambda_{\mathrm{ThB}}} \right. \\ &\quad \left. - \left(\frac{N_{ThB2} \lambda_{\mathrm{ThB}}}{\lambda_{\mathrm{ThC}} - \lambda_{\mathrm{ThB}}} - N_{\mathrm{ThC2}} \right) e^{-\lambda_{\mathrm{ThC}} \left(iT - \frac{1}{2} T \right)} \right] \end{aligned} \tag{13}$$

$$\begin{aligned}\frac{n_{\mathrm{RaC}}(i)}{T} &= EA_{\mathrm{RaC}}\left(iT-\frac{1}{2}T\right)\\ &= E\lambda_{\mathrm{RaC}}\left\{\frac{-\left(\frac{\lambda_{\mathrm{RaA}}N_{\mathrm{RaA2}}}{\lambda_{\mathrm{RaB}}-\lambda_{\mathrm{RaA}}}-N_{\mathrm{RaB2}}\right)\lambda_{\mathrm{RaB}}e^{-\lambda_{\mathrm{RaB}}\left(iT-\frac{1}{2}T\right)}}{\lambda_{\mathrm{RaC}}-\lambda_{\mathrm{RaB}}}\right.\\ &+\frac{\frac{N_{\mathrm{RaA2}}}{\lambda_{\mathrm{RaB}}-\lambda_{\mathrm{RaA}}}\lambda_{\mathrm{RaA}}\lambda_{\mathrm{RaB}}e^{-\lambda_{\mathrm{RaA}}\left(iT-\frac{1}{2}T\right)}}{\lambda_{\mathrm{RaC}}-\lambda_{\mathrm{RaA}}}\\ &+\left[N_{\mathrm{RaC2}}+\frac{\left(\frac{\lambda_{\mathrm{RaA}}N_{\mathrm{RaA2}}}{\lambda_{\mathrm{RaB}}-\lambda_{\mathrm{RaA}}}-N_{\mathrm{RaB2}}\right)\lambda_{\mathrm{RaB}}}{\lambda_{\mathrm{RaC}}-\lambda_{\mathrm{RaB}}}\right.\\ &\left.\left.-\frac{\frac{\lambda_{\mathrm{RaA}}N_{\mathrm{RaA2}}}{\lambda_{\mathrm{RaB}}-\lambda_{\mathrm{RaA}}}\lambda_{\mathrm{RaB}}}{\lambda_{\mathrm{RaC}}-\lambda_{\mathrm{RaA}}}\right]e^{-\lambda_{\mathrm{RaC}}\left(iT-\frac{1}{2}T\right)}\right\}\end{aligned} \tag{14}$$

$$\begin{aligned}\frac{n_{\mathrm{RaA+ThC}}(i)}{T} &= E\left\{A_{\mathrm{RaA}}\left(iT-\frac{1}{2}T\right)+0.36A_{\mathrm{ThC}}\left(iT-\frac{1}{2}T\right)\right\}\\ &= E\left\{N_{\mathrm{RaA2}}e^{-\lambda_{\mathrm{RaA}}\left(iT-\frac{1}{2}T\right)}\right.\\ &+0.36\lambda_{\mathrm{ThC}}\left[\frac{\lambda_{\mathrm{ThB}}N_{\mathrm{ThB2}}e^{-\lambda_{\mathrm{ThB}}\left(iT-\frac{1}{2}T\right)}}{\lambda_{\mathrm{ThC}}-\lambda_{\mathrm{ThB}}}\right.\\ &\left.\left.-\left(\frac{N_{\mathrm{ThB2}}\lambda_{\mathrm{ThB}}}{\lambda_{\mathrm{ThC}}-\lambda_{\mathrm{ThB}}}-N_{\mathrm{ThC2}}\right)e^{-\lambda_{\mathrm{ThC}}\left(iT-\frac{1}{2}T\right)}\right]\right\}\end{aligned} \tag{15}$$

where E denotes the detection efficiency of the detector for alpha particles, i denotes the counting cycle of alpha particles, and $iT-1/2T$ denotes the midpoint time of the ith counting cycle.

Based on Eqs. (13, 14, and 15), the number of atoms (N_{RaA2}, N_{RaB2}, N_{RaC2}, N_{ThB2}, and N_{ThC2}) can be determined through the nonlinear fit of the experimental data, and the calculation processes are as follows:

(1) N_{ThB2} and N_{ThC2} can be obtained using Eq. (13) to perform a nonlinear fitting of the experimental data for $(n_{\mathrm{ThC}}(i))/t$.
(2) By substituting the value of N_{ThC2} into Eq. (15) and employing nonlinear fitting of the experimental data for $(n_{\mathrm{RaA}}(i))/t$ using Eq. (15), N_{RaA2} can be obtained as:
(3) By inserting N_{RaA2} into Eq. (14) and utilizing the nonlinear fitting of the experimental data for $(n_{\mathrm{RaA+ThC}})/t$ using Eq. (14), N_{RaB2} and N_{RaC2} are determined.

After obtaining the values of N_{RaA2}, N_{RaB2}, N_{RaC2}, N_{ThB2}, and N_{ThC2}, the activity concentrations of RaA, RaB, RaC, ThB, and ThC in air can be deduced by reversing Eqs. (1 and 2).

2.3 Limit of detection and error analysis

The net signal level (instrument response) above which an observed signal can be reliably recognized as detected is defined as the critical limit (L_{C}). This indicates that a particular nuclide is definitely present in the sample [35]. The same values are defined in ISO standard 11,929, but the mathematical assessment of ionizing radiation measurement utilizes Bayesian statistics, which comprise calculations with conditional probabilities [37–40]. According to ISO standard 11,929, the decision threshold or critical level (L_{C}), assuming small number of background counts (C_{b}), was calculated using the following formula:

$$L_{\mathrm{C}}(\text{ in counts }) = k\cdot\sqrt{2\cdot\left(C_{\mathrm{b}}+1\right)} \tag{16}$$

where k denotes the confidence factor ($k=1.645$ at confidence level of 95%).

The uncertainties in the activity concentration (σ_{C_i}) can be expressed by Eq. (17) [37–40]. It is composed of the uncertainty of counts Ni, detection efficiency E, filtration efficiency G, and flow rate Q, whereas the uncertainties of sampling and counting times are usually ignored.

$$\begin{aligned}\sigma_{C_i} = &\left[\left(\frac{\partial C_i}{\partial N_i}\right)^2\sigma_{N_i}^2+\left(\frac{\partial C_i}{\partial E}\right)^2\sigma_E^2+\left(\frac{\partial C_i}{\partial G}\right)^2\sigma_G^2\right.\\ &\left.+\left(\frac{\partial C_i}{\partial Q}\right)^2\sigma_Q^2\right]^{\frac{1}{2}}\end{aligned} \tag{17}$$

where σ_{C_i} ($i=1,2,3,4,5$) denotes the uncertainties of activity concentration of RaA, RaB, RaC, ThB, and ThC, σ_E denotes the standard uncertainty of the detection efficiency, σ_G denotes the standard uncertainty of the filtration efficiency, and σ_Q denotes the standard uncertainty of the flow rate.

3 Results and discussion

Several experiments based on air filtration of ^{222}Rn and ^{220}Rn progeny concentrations were conducted in mixed ^{222}Rn and ^{220}Rn chamber at the University of South China. This chamber is made of stainless steel and has an inner effective volume of 3 m^3. It is connected to the gas path, allowing continuous compensation for ^{222}Rn and ^{220}Rn progeny. The flow rate for each sampling experiment was calibrated to 15 ± 0.45 L min^{-1} using a soap bubble flowmeter, and the sampling duration lasts for

fifteen minutes. The volume of the sampled gas occupies only 8% of the entire chamber volume, and continuous progeny replenishment ensures relative stability in the measurement environment. The sampling filter membrane is a 0.8 µm Millipore AA-type microfiltration membrane with a diameter of 25 mm. The filtration efficiency of the filter membrane is 0.990 ± 0.002, and its self-absorption is considered negligible. Aerosols are generated using an aerosol generator, and an aerosol electrometer, produced by TSI Incorporated, is used to monitor the number concentration of aerosols. The aerosol concentration varied from 8×10^3 cm^{-3} to 10×10^3 cm^{-3} in the experiments.

The measurements were taken at 27 °C and 75% relative humidity (RH) using an alpha spectrometer. This alpha spectrometer, manufactured by ORTEC Corporation, utilizes an ion-implanted surface-passivated silicon detector with an 900 mm^2 probe. It realizes an energy resolution of 20 keV under a vacuum pressure below 1000 mTorr. Under these measurement conditions, the alpha particles exhibit a longer range and minimal energy loss with a measurement distance of only 1 mm and no spectral broadening occurs. Consequently, the distinct characteristic energy peaks of ^{222}Rn and ^{220}Rn progenies can be clearly distinguished using 1024 channels. The alpha spectrometer calibrates its alpha detection efficiency (E) using a ^{241}Am electroplated surface source. The resulting mean value for E was 33.3%, accompanied by 2.0% uncertainty.

To compare the accuracy of the results obtained from the proposed model with those of the total count method presented in Ref. [25], the measurement cycle of the alpha spectrometer was set to 1 min and lasted for more than 560 min. This method can provide alpha counts at different time intervals as required by both methods. The automatic measurement process using an alpha spectrometer was realized by writing JOB files in MAESTRO software, which can display and store real-time measurement data. A portion of the measured data is presented in Fig. 3.

Considering the impact of statistical fluctuations on net alpha counts and the influence of measurement intervals and cycle periods on the standard error of the calculated results, nine short counting cycles (i) were selected consecutively from the beginning of the measurement, with each counting cycle (T) set to 10 min. The background count for a measurement time of 90 min was 31 ± 3. According to Eq. (17), the critical limit (L_C) of the alpha spectrometer for the counts obtained using the new method was 13. The net counts of alpha particles emitted from ^{222}Rn and ^{220}Rn progeny were recorded based on alpha particle energies of 8.78 MeV, 7.69 MeV, and 6.0 MeV, and their ROI-1 (8.78 MeV), ROI-2 (7.69 MeV), and ROI-3 (6.0 MeV) were 2–6.3 MeV, 6.3–8 MeV, and 8–10 MeV, respectively.

Origin software (OriginLab Corporation) enables users to customize functions for nonlinear fitting, ensuring the accurate modeling of complex data relationships. This capability provides enhanced precision and adaptability in nonlinear

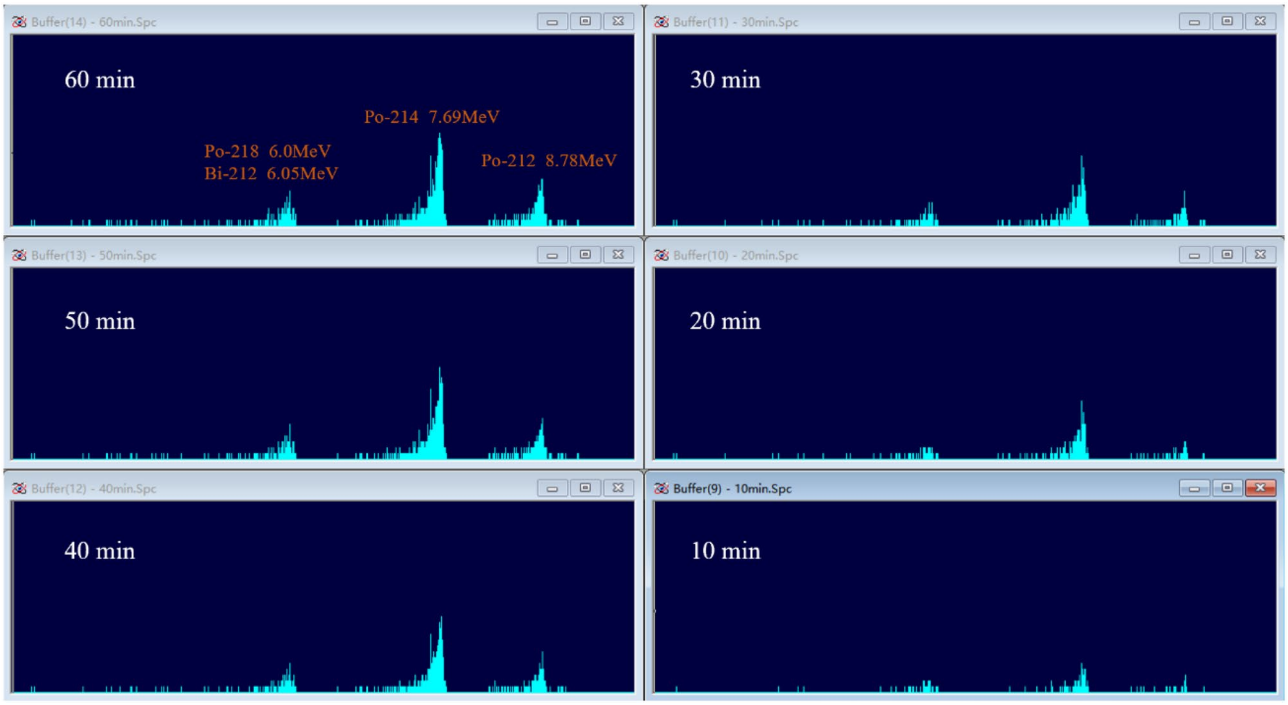

Fig. 3 (Color online) Alpha counts with energies of 6.0 MeV, 7.69 MeV, and 8.78 MeV measured via display in Maestro software

data analysis, making it a widely used tool for calculating ^{222}Rn and ^{220}Rn concentrations [41, 42]. The fitting method is based on the radioactive decay law that uses nonlinear fitting by Origin2021 and returns the best-fit parameters and their statistical errors for each free parameter fitted. In this study, the fitted parameters N_{RaA2}, N_{RaB2}, N_{RaC2}, N_{ThB2}, and N_{ThC2} are the primary focus. Figure 4 illustrates three experimental results for the net alpha particle counts measured by the alpha spectrometer, which varies with the measurement period. The alpha counts from RaA and ThC, both around 6 MeV, were counted, and the results of the three experiments are shown in Fig. 4b, e, and h. Given significantly shorter half-life of RaA when compared with that of ThC, their alpha counts initially decreased rapidly, followed by a slow rise. The alpha counts from ThC and RaC are presented in Fig. 4a, d, g, and c–i, respectively. According to Eqs. (13, 14 and 15), the number of atoms of RaA, RaB, RaC, ThB, and ThC on the filter membrane (N_{RaA2}, N_{RaB2}, N_{RaC2}, N_{ThB2}, and N_{ThC2}) at the initiation of alpha spectrometer measurement was derived through nonlinear fitting of alpha counts with energies of 6.0 MeV, 7.69 MeV, and 8.78 MeV using Origin2021 software. By inserting the values of N_{RaA2}, N_{RaB2}, N_{RaC2}, N_{ThB2}, and N_{ThC2} into Eqs. (1 and 2) using MATLAB, the concentrations of ^{222}Rn and ^{220}Rn progenies in the air can be obtained, and the detailed data are listed in Table 1.

Only minor changes were observed in the number of aerosol particles and environmental parameters, and the sources of ^{222}Rn and ^{220}Rn remained unchanged during the process of conducting the three measurement experiments. Table 1 shows that R^2 for N_{ThB2} and N_{ThC2} in the first experiment, as well as for N_{RaA2} in the second and third experiments, are not satisfactory. This may be due to the impact of statistical fluctuations in counts over consecutive cycles. However, based on the results of the three experiments, the differences observed in the concentrations of the same types of ^{222}Rn and ^{220}Rn progeny calculated using the same method in the three experiments may be attributed to minor variations in the quantity of aerosol particles suspended in the environment and other environmental parameters. The poor goodness of fit of one of the nuclides slightly impacts the overall experimental results.

Table 1 Three experimental results of simultaneous measurements of ^{222}Rn and ^{220}Rn progeny concentrations ($k = 1$)

Experiment number	Progeny	The number of atoms on the filter membrane	R^2	Activity concentration in air (Bq m^{-3})
1	N_{RaA2}	229 ± 19	0.93	17.234 ± 1.537
	N_{RaB2}	2270 ± 133	0.96	3.845 ± 0.364
	N_{RaC2}	1220 ± 97	0.96	2.809 ± 0.362
	N_{ThB2}	30955 ± 2244	0.67	2.539 ± 0.199
	N_{ThC2}	1646 ± 123	0.67	1.298 ± 0.124
2	N_{RaA2}	308 ± 46	0.63	23.175 ± 3.495
	N_{RaB2}	4053 ± 124	0.99	7.569 ± 0.491
	N_{RaC2}	2499 ± 93	0.99	6.098 ± 0.384
	N_{ThB2}	60926 ± 4340	0.80	4.997 ± 0.386
	N_{ThC2}	2365 ± 229	0.80	1.729 ± 0.225
3	N_{RaA2}	275 ± 45	0.65	20.665 ± 3.453
	N_{RaB2}	2470 ± 122	0.97	4.006 ± 0.446
	N_{RaC2}	1358 ± 89	0.97	3.178 ± 0.338
	N_{ThB2}	38466 ± 1593	0.92	3.155 ± 0.161
	N_{ThC2}	1550 ± 84	0.92	1.146 ± 0.088

The ^{222}Rn and ^{220}Rn progeny concentrations calculated using the new method were compared with those obtained using the total count method presented in the literature [25]. According to [23], the second set of counting intervals was selected for application to the total count method. The first and second sets of counting intervals were (1,4), (5,20), (21,40), (150,250), (360,560) and (2,5), (6,20), (21,30), (200,300), (360,560) min, respectively. The alpha counts from these two measurement intervals of the three experiments were input into the model of the total count method. Furthermore, a comparison of the results for the activity concentrations of ^{222}Rn and ^{220}Rn progeny in air, calculated via the new method and total count method, is shown in Fig. 5.

Figure 5 illustrates that the activity concentrations of ^{222}Rn and ^{220}Rn progeny, calculated using the new method, are all positive, whereas the activity concentrations of RaB, RaC, and ThB, calculated using the total count method with two sets of counting intervals, exhibited negative values. The occurrence of negative concentration of ^{222}Rn and ^{220}Rn progeny is not in accordance with reality. The primary reason may be that the accuracy of calculating comparatively lower progeny concentrations in the air using the total count method is insufficient, coupled with the statistical fluctuations in the counts as well as the overlapping effect between different spectra during long-term measurements. The total count method in Ref. [25] utilizes the radioactive decay law of alpha particles within five different time intervals (560 min) to obtain the concentrations of ^{222}Rn and ^{220}Rn progeny in the air. Compared to the total count method, the advantage of the new method lies in distinguishing nuclides with overlapping spectra by utilizing the alpha particle counts of non-overlapping spectra within consecutive measurement cycles (90 min). This enables the distinction of nuclides with different energy spectra and facilitates nonlinear fitting based on the radioactive decay law to determine the concentration of each progeny. Moreover, the measurement time is reduced by 84%.

Given the close proximity of the alpha energies emitted by RaA and ThC, both around 6 MeV, their counts were not distinguished in each experiment, but were counted together. For alpha counts with energies of 6 MeV, the quantity of

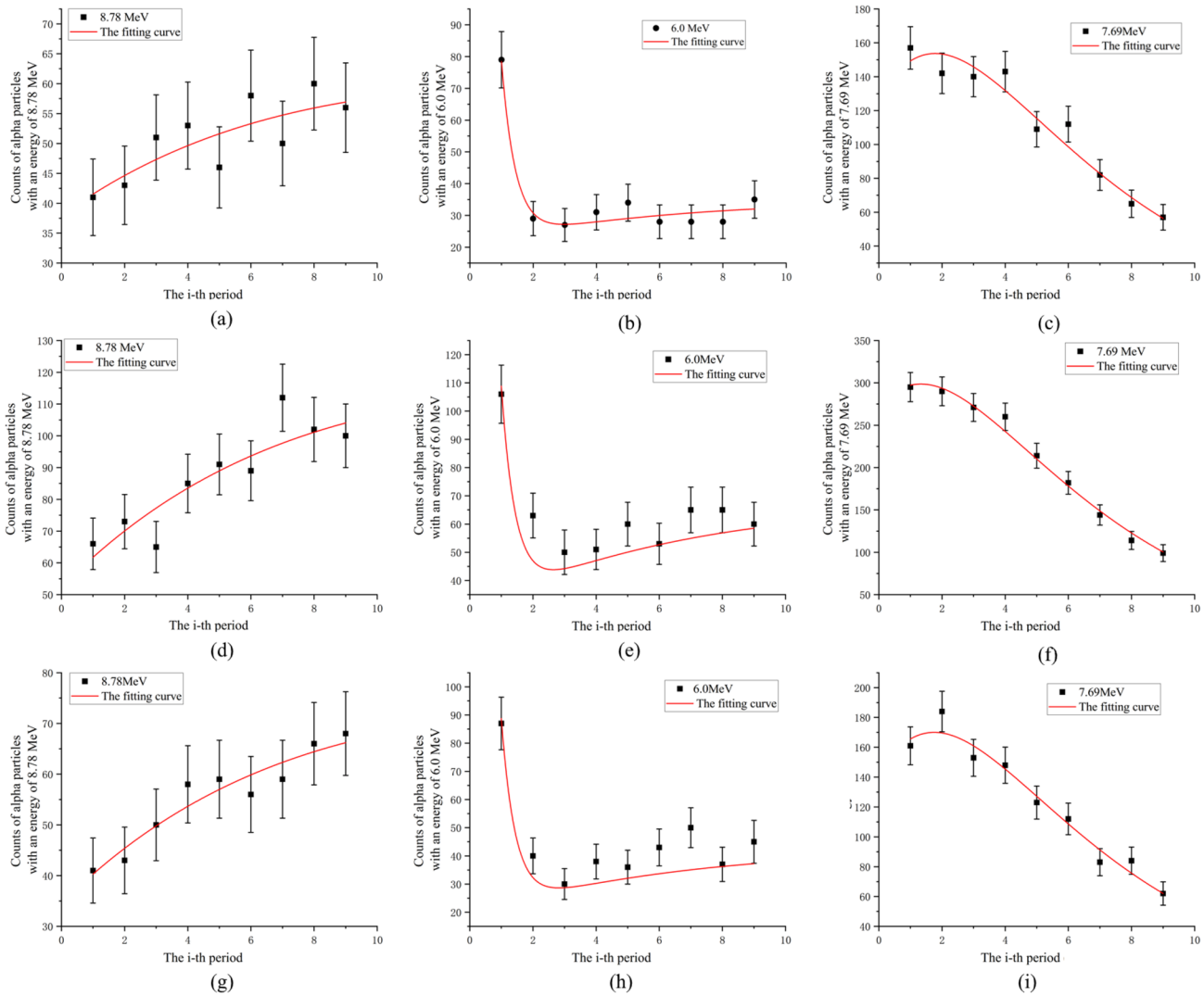

Fig. 4 (Color online) Three experimental results of net alpha particle counts measured by the alpha spectrometer (with energies of 8.78 MeV, 6.0 MeV, and 7.69 MeV) vary with the measurement period: the first experiment (a, b, c), second experiment (d, e, f), and third experiment (g, h, i). *i* represents the *i*th measurement period, with each cycle lasting 10 min

RaA will decay rapidly within a short period because of the much shorter half-life of RaA when compared to that of ThC. When the total count method with long time intervals is employed, the activity concentration of RaA in air may have been underestimated, leading to an overestimation of the activity concentration of ThC. However, by utilizing the continuous counts of the 8.78 MeV ThC' spectrum within consecutive cycles and the determined decay branching ratio, it is easier to distinguish between the spectral counts of RaA and ThC. Hence, the concentration of RaA, calculated using the total count method, is lower than that determined by the new method, whereas ThC exhibits a higher concentration when compared to the calculation by the new method, as shown in Fig. 5. Although the fitting quality of some curves in Fig. 4 is not optimal, it has minimal effect on the overall accuracy of the experiments. Detailed data are listed in Table 2.

Considering that the relative uncertainty of the detection efficiency σ_E/E is ± 2.0%, the relative uncertainty of the flow rate σ_Q/Q is ± 3.0%, and the statistical uncertainty, relative uncertainty of radon progeny concentrations provided by the new methods are all within ± 16%, and those of the thoron progeny concentrations are within ± 13%. These uncertainties are significantly lower than those calculated using the total count method. Owing to the lower concentrations of measured progeny, there are significant statistical fluctuation errors, but the statistical errors of progeny concentrations calculated by the new method are within a reasonable range using the 10-min average as the measurement

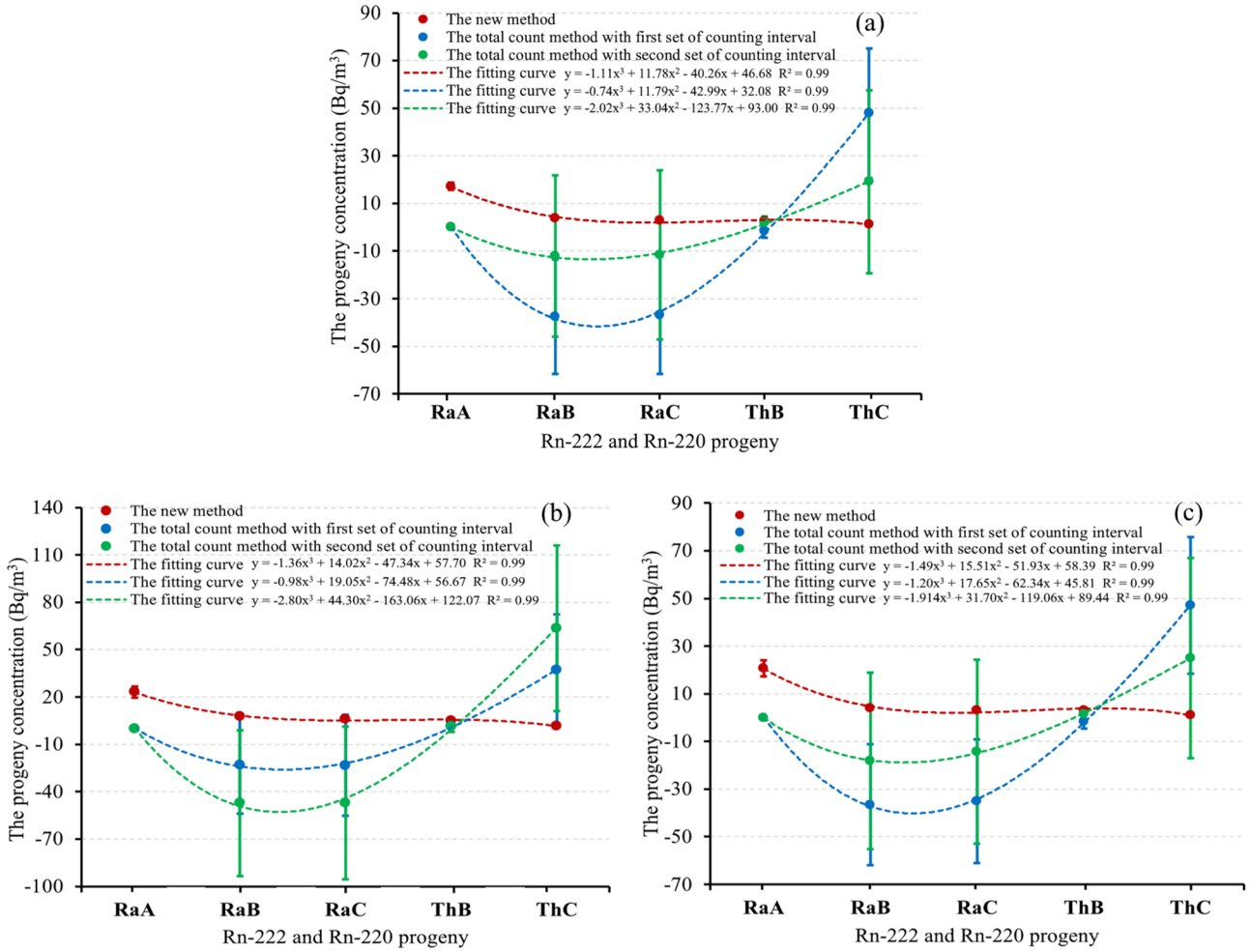

Fig. 5 (Color online) Three experimental results of simultaneous measurements of ^{222}Rn and ^{220}Rn progeny concentrations: **a** first experiment; **b** second experiment; and **c** third experiment. (The counting interval of the new method was 90 min; the first and second sets of counting intervals are (1, 4), (5, 20), (21, 40), (150, 250), (360, 560), and (2, 5), (6, 20), (21, 30), (200, 300), (360, 560) min)

value for one cycle. A low measurement uncertainty is more meaningful for accurate measurements.

Given the negative values observed in the concentration of ^{222}Rn progeny calculated using the total count method in the three experiments, the equilibrium equivalent radon concentration was not considered. The ^{220}Rn decay product concentrations were measured in terms of equivalent concentrations (EEC_{Tn}), as provided by the following relations [43]:

$$EEC_{\mathrm{Tn}} = 0.913\left(C_{^{212}\mathrm{Pb}}\right) + 0.087\left(C_{^{214}\mathrm{Bi}}\right) \tag{18}$$

where $C_{^{212}\mathrm{Pb}}$ and $C_{^{214}\mathrm{Bi}}$ are the activity concentrations in Bq/m^3.

Table 3 shows that the EEC_{Tn} trends calculated by both methods are consistent, with EEC_{Tn} in the second experiment being slightly higher than those in the first and third experiments. The lower limit values of the standard errors calculated using the total method for the three experiments were negative, which is inconsistent with the actual situation. However, the values of EEC_{Tn} calculated using the new method are within the range of the standard errors of those calculated using the total method, with the relative standard deviation of EEC_{Tn} ranging from 5% to 8%. Given the measurement uncertainties associated with different methods and fluctuations in progeny concentrations across various sampling processes, it can be confirmed that consistency was achieved. The experiments were conducted at relatively low progeny concentrations of ^{222}Rn and ^{220}Rn. The results obtained by comparing the two methods demonstrate that the proposed method has significant advantages.

Table 2 Comparison of results from two methods in experiments of simultaneously measuring ^{222}Rn and ^{220}Rn progeny concentrations ($k = 1$)

Experiment number	Progeny	Activity concentration(the new method) (Bq m^{-3})	Activity concentration (the total count method with first set of time internals) (Bq m^{-3})	Activity concentration (the total count method with second set of time internals) (Bq m^{-3})
1	N_{RaA2}	17.234 ± 1.537	0.009 ± 0.006	0.002 ± 0.005
	N_{RaB2}	3.845 ± 0.364	− 37.547 ± 24.026	− 12.112 ± 33.835
	N_{RaC2}	2.809 ± 0.362	− 36.851 ± 24.640	− 11.598 ± 35.417
	N_{ThB2}	2.539 ± 0.199	− 1.521 ± 2.850$	1.915 ± 2.564
	N_{ThC2}	1.298 ± 0.124	47.867 ± 27.200	19.166 ± 38.491
2	N_{RaA2}	23.175 ± 3.495	0.007 ± 0.008	0.008 ± 0.007
	N_{RaB2}	7.569 ± 0.491	− 22.951 ± 31.027	− 47.278 ± 46.204
	N_{RaC2}	6.098 ± 0.384	− 23.383 ± 31.980	− 47.063 ± 48.296
	N_{ThB2}	4.997 ± 0.386	1.601 ± 3.693	1.298 ± 3.497
	N_{ThC2}	1.729 ± 0.225	37.305 ± 35.205	63.546 ± 52.534
3	N_{RaA2}	20.665 ± 3.453	0.010 ± 0.006	0.003 ± 0.005
	N_{RaB2}	4.006 ± 0.446	− 36.594 ± 25.362	− 18.219 ± 36.999
	N_{RaC2}	3.178 ± 0.338	− 35.076 ± 25.994	− 14.361 ± 38.546
	N_{ThB2}	3.155 ± 0.161	− 1.552 ± 3.007	1.499 ± 2.795
	N_{ThC2}	1.146 ± 0.088	47.124 ± 28.702	24.997 ± 41.981

Table 3 Comparison of results of EEC_{Tn} from two methods ($k = 1$)

Experiment number	EEC_{Tn} calculated by the new method (Bq m^{-3})	EEC_{Tn} calculated by the total method with second set of internals (Bq m^{-3})
1	2.431 ± 0.194	3.416 ± 11.615
2	4.713 ± 0.375	6.714 ± 15.851
3	2.980 ± 0.156	3.543 ± 12.667

4 Conclusion

The concentrations of ^{222}Rn and ^{220}Rn progeny in the environment pose a risk of natural radiation exposure to the public. A novel mathematical model, utilizing a nonlinear fitting method based on the radioactive decay law, is proposed for the simultaneous measurement of ^{222}Rn and ^{220}Rn progeny concentrations in air. The experimental findings indicated that ^{222}Rn and ^{220}Rn progeny concentrations determined using the new method were all positive and exhibited a closer alignment with the actual conditions than the total count method. With their relative uncertainties within ± 16%, it can be confirmed that consistency has been achieved. Moreover, the measurement time was reduced by 84%. This novel approach exhibited improved efficacy in discriminating alpha particles with analogous energies emitted from RaA and ThC, both approximately 6 MeV, consequently yielding results with heightened accuracy. The method proposed in this study has greater potential advantages for the faster measurement of relatively low concentrations of ^{222}Rn and ^{220}Rn progeny in air.

Author Contributions All authors contributed to the study conception and design. Material preparation, data collection, and analysis were performed by Jian Shan, Yan-Liang Tan, Zhong-Kai Fan, Shou-Kang Qiu, Hui Yang, Jia-Le Sun, Hao-Xuan Li, and Xiang-Ming Cai. The first draft of the manuscript was written by Zhong-Kai Fan, and all authors commented on previous versions of the manuscript. All authors read and approved the final manuscript.

Data availability The data that support the findings of this study are openly available in Science Data Bank at https://cstr.cn/31253.11.sciencedb.12735 and https://www.doi.org/10.57760/sciencedb.12735.

Declarations

Conflict of interest The authors declare that they have no conflict of interest.

References

1. Y.J. Ju, Y.H. Ryu, H.C. Jang et al., A study on concentration measurements of radon-222 (uranium series) and radon-220 (thoron series) emitted to the atmosphere from tex (cementitious), red brick, and ecocarat among construction materials. J. Korean Phys. Soc. **60**, 1177–1186 (2012). https://doi.org/10.3938/jkps.60.1177

2. M. Xia, Y.J. Ye, S.Y. Liu, Numerical simulations for radon migration and exhalation behavior during measuring radon exhalation rate with closed-loop method. Nucl. Sci. Tech. **35**, 9 (2024). https://doi.org/10.1007/s41365-024-01362-z
3. M. Kaur, A. Kumar, R. Mehra et al., Assessment of radon, thoron, and their progeny concentrations in the dwellings of Shivalik hills of Jammu and Kashmir, India. Environ. Geochem. Health (2020). https://doi.org/10.1007/s10653-020-00767-0
4. S. Abdullahi, A.F. Ismail, S. Samat, Radiological characterization of building materials used in Malaysia and assessment of external and internal doses. Nucl. Sci. Tech. **30**, 46 (2019). https://doi.org/10.1007/s41365-019-0569-3
5. P. Pagelkopf, J. Porstendörfer, Neutralisation rate and the fraction of the positive ^{218}Po-clusters in air. Atmos. Environ. **37**(8), 1057–1064 (2003). https://doi.org/10.1016/S1352-2310(02)00997-4
6. A. Reineking, K.H. Becker, J. Porstendörfer, Measurements of the unattached fractions of radon daughters in houses. Sci. Total Environ. **45**, 261–270 (1985). https://doi.org/10.1016/0048-9697(85)90227-X
7. M. Ramamurthi, P.K. Hopke, On improving the validity of wire screen "unattached'' fraction Rn daughter measurements. Health Phys. **56**(2), 189–194 (1989). https://doi.org/10.1097/00004032-198902000-00006
8. A. Koli, P. Khandare, M. Joshi et al., Estimating back to front ratio of wire screen for measurement of thoron decay products. J. Environ. Radioact. **151**, 341–347 (2016). https://doi.org/10.1016/j.jenvrad.2015.10.003
9. L.F. Li, R. Chen, S.M. Zhou et al., Evaluation of correlation between PM2. Five and the radon-progeny equilibrium factor in the radon chamber. Nucl. Sci. Tech. **29**(10), 151 (2018). https://doi.org/10.1007/s41365-018-0481-2
10. G.M. Kendall, T.J. Smith, Doses to organs and tissues from radon and its decay products. J. Radiol. Prot. **22**(4), 389 (2002). https://doi.org/10.1088/0952-4746/22/4/304
11. S. Sharma, A. Kumar, R. Mehra et al., Assessment of progeny concentrations of ^{222}Rn/^{220}Rn and their related doses using deposition-based direct progeny sensors. Environ. Sci. Pollut. Res. **25**, 11440–11453 (2018). https://doi.org/10.1007/s11356-018-1414-7
12. C. Zhao, J. Liu, Y. Chen et al., Thoron gas measurement using airflow-through scintillation cell with consideration of progeny deposition. Atmosphere **14**(5), 831 (2023). https://doi.org/10.3390/atmos14050831
13. Z. Fan, T. Hu, X. Cai et al., Development of a novel low-pressure scintillation cell with ZnS (Ag)-coated clapboard for ^{220}Rn measurement. Appl. Radiat. Isot. **203**, 111107 (2023). https://doi.org/10.1016/j.apradiso.2023.111107
14. F. Qin, H. Luo, Z. He, K. Lu et al., Counting of alpha particle tracks on imaging plate based on a convolutional neural network. Nucl. Sci. Tech. **34**(3), 37 (2023). https://doi.org/10.1007/s41365-023-01190-7
15. D. Fan, W. Zhuo, B. Chen et al., Uncertainty of an automatic system for counting alpha tracks on CR-39. Nucl. Sci. Tech. **28**(11), 164 (2017). https://doi.org/10.1007/s41365-017-0314-8
16. Z. Fan, J. Shan, F. Lin et al., Developing a radon monitor for simultaneous measurement of ^{222}Rn and ^{220}Rn with less influence of humidity based on electrostatic collection and CR-39 detector. Nucl. Instrum. Methods Phys. Res. A **1052**, 168285 (2023). https://doi.org/10.1016/j.nima.2023.168285
17. Y. Wang, Y. Liu, B. Wu et al., Experimental investigation on the radiation background inside body counters. Nucl. Sci. Tech. **33**(2), 20 (2022). https://doi.org/10.1007/s41365-022-01004-2
18. R. Xie, F. Lin, H. Li et al., Development of the ultra-high sensitivity radon monitor based on electrostatic collection method. JINST **18**(11), P11020 (2023). https://doi.org/10.1088/1748-0221/18/11/P11020
19. AlphaSuite User's Manual, https://www.ortec-online.com.cn/productscn/radiochemistry-health-physics-research-industrial/alpha-spectroscopy/spectrometers/alpha-suite
20. G. Jia, J. Jia, Determination of radium isotopes in environmental samples by gamma spectrometry, liquid scintillation counting and alpha spectrometry: a review of analytical methodology. J. Environ. Radioact. **106**, 98–119 (2012). https://doi.org/10.1016/j.jenvrad.2011.12.003
21. N.H. Harley, B.S. Pasternack, Experimental absorption applied to lung dose from thoron daughters. Health Phys. **24**(4), 379–386 (1973)
22. C. Zhang, D. Luo, A method for measuring mixed radon and thoron daughters and analyzing data by weighted least squares. Radiat. Prot. **3**(2), 98–110 (1983). **(in Chinese)**
23. C. Zhang, D. Luo, Measurement of mixed radon and thoron daughter concentrations in air. Nucl. Instrum. Methods Phys. Res. **215**(3), 481–488 (1983). https://doi.org/10.1016/0167-5087(83)90482-9
24. J.M. Stajic, D. Nikezic, Analysis of radon and thoron progeny measurements based on air filtration. Radiat. Prot. Dosim. **163**(3), 333–340 (2015). https://doi.org/10.1093/rpd/ncu183
25. J.M. Stajic, D. Nikezic, The accuracy of radon and thoron progeny concentrations measured through air filtration. J. Environ. Radioact. **140**, 50–58 (2015). https://doi.org/10.1016/j.jenvrad.2014.11.002
26. J.W. Thomas, Measurement of radon daughters in air. Health Phys. **23**(6), 783–789 (1972). https://doi.org/10.1097/00004032-197212000-00004
27. A. Khan, A. Busigin, C.R. Phillips, An optimized scheme for measurement of the concentrations of the decay products of radon and thoron. Health Phys. **42**(6), 809–826 (1982). https://doi.org/10.1097/00004032-198206000-00006
28. J. Bigu, G. Vandrish, Radon (thoron) daughter measurements with an automated, programmable. Radiation monitor. Environ. Monit. Assess. **6**, 59–70 (1986). https://doi.org/10.1007/BF00394288
29. N.P. Thiessen, Alpha particle spectroscopy in radon/thoron progeny measurements. Health Phys. **67**(6), 632–640 (1994). https://doi.org/10.1097/00004032-199412000-00006
30. G.D. Kerr, M.T. Ryan, P.T. Perdue, Measurement of airborne concentrations of radon-220 daughter products by alpha-particle spectrometry (No. CONF-780110-1). Oak Ridge National Lab., Tenn.(USA). https://www.osti.gov/servlets/purl/5168863
31. K. Peng, H. Wang, J. Yang et al., Improvement and verification of new measurement methods for radon and thoron progeny activity concentration based on alpha spectrometry analysis. Radiat. Meas. **172**, 107068 (2024). https://doi.org/10.1016/j.radmeas.2024.107068
32. Y. Xu, X. Tuo, R. Shi et al., Monte Carlo simulation and influencing factors of detection efficiency of PIPS-α spectrometer. High Power Laser Part. Beams **29**(10), 106002 (2017). ((**in Chinese**))
33. S. Pommé, B.C. Marroyo, Improved peak shape fitting in alpha spectra. Appl. Radiat. Isot. **96**, 148–153 (2015). https://doi.org/10.1016/j.apradiso.2014.11.023
34. F. Ambrosino, Study on a peak shape fitting model for the analysis of alpha-particle spectra. Appl. Radiat. Isot. **159**, 109090 (2020). https://doi.org/10.1016/j.apradiso.2020.109090
35. Y. Tan, H. Yuan, K.J. Kearfott, Energy-dependent etching-related impacts on CR-39 alpha detection efficiency for the ^{222}Rn and ^{220}Rn decay chains. JINST **13**(04), T04005 (2018). https://doi.org/10.1088/1748-0221/13/04/T04005
36. Z. Fan, R. Xie, X. Cai et al., Determining the calibration factor of ^{220}Rn by low-pressure scintillation cell. Metrologia (2023). https://doi.org/10.1088/1681-7575/acdd08

37. L.A. Currie, Limits for qualitative detection and quantitative determination. Appl. Radiochem. Anal. Chem. **40**(3), 586–593 (1968). https://doi.org/10.1021/ac60259a007
38. ISO, Determination of the Characteristic Limits (Decision Threshold, Detection Limit and Limits of the Confidence Interval) for the measurement of ionizing radiation. in *Parts 1. (International Organization for Standardization*, (Geneva, 2019), pp. 2–3
39. IAEA. International Atomic Energy Agency, Determination and Interpretation of Characteristic Limits for Radioactivity Measurements: Decision Threshold, Detection Limit and Limits of the Confidence Interval. in *IAEA Analytical Quality in Nuclear Application* Series No., vol. 48. IAEA, Vienna (2017)
40. E.M. El Afifi, M.A. Hilal, M.F. Attallah, Performance characteristics and validation of alpha particle spectrometers for radiometric analysis of natural and anthropogenic radionuclides of environmental impacts. Appl. Radiat. Isot. **168**, 109548 (2021). https://doi.org/10.1016/j.apradiso.2020.109548
41. S. Liu, Z. Fan, R. Xie et al., Development of a novel method for rapid and accurate determination of Ra-226 activity in soil by NaI (TI) spectrometer. Radiat. Phys. Chem. **218**, 111654 (2024). https://doi.org/10.1016/j.radphyschem.2024.111654
42. J. Yang, H. Busen, H. Scherb et al., Modeling of radon exhalation from soil influenced by environmental parameters. Sci. Total Environ. **656**, 1304–1311 (2019). https://doi.org/10.1016/j.scitotenv.2018.11.464
43. ICRP (International Commission on Radiological Protection) Limits of inhalation of radon daughters for workers. ICRP Publication-32, Annals Vol. 6(1). (Pergamon Press, Oxford, 1981)